

Iron Sulfido Derivatives of the Fullerenes C₆₀ and C₇₀

Mark D. Westmeyer, Thomas B. Rauchfuss,* and Atul K. Verma

School of Chemical Sciences, University of Illinois, Urbana, Illinois 61801

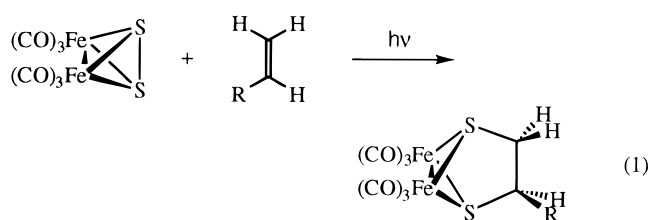
Received June 18, 1996[⊗]

Toluene solutions of C₆₀ react upon UV irradiation with Fe₂S₂(CO)₆ to give C₆₀[S₂Fe₂(CO)₆]_n where n = 1–6. C₆₀[S₂Fe₂(CO)₆]_n where n = 1–3 have been isolated and characterized. Crystallographic studies of C₆₀S₂Fe₂(CO)₆ show that the S–S bond of the Fe₂ reagent is cleaved to give a dithiolate with idealized C_{2v} symmetry. The addition occurred at a 6,6 fusion, and the metrical details show that the Fe₂ portion of the molecule resembles C₂H₄S₂Fe₂(CO)₆. IR spectroscopic measurements indicate that the Fe₂(CO)₆ subunits in the multiple-addition species (n > 1) interact only weakly. UV–vis spectra of the adducts show a shift to shorter wavelength with addition of each S₂Fe₂(CO)₆ unit. Photoaddition of the phosphine complex Fe₂S₂(CO)₅(PPh₃) to C₆₀ gave C₆₀–[S₂Fe₂(CO)₅(PPh₃)]_n, where n = 1–3. ³¹P{¹H} NMR studies show that the double adduct consists of multiple isomers. Photoaddition of Fe₂S₂(CO)₆ to C₇₀ gave a series of adducts C₇₀[S₂Fe₂(CO)₆]_n where n = 1–4. HPLC analyses show one, four, and three isomers for the adducts, respectively.

Introduction

Metal complexes figure prominently in the array of reagents that attack the C₆₀, C₇₀, and C₈₄ cages.¹ Fullerenes interact with metals most commonly via direct metal–cage bonding. Cases where the fullerene binds to ligands are rare, although noteworthy examples are provided by Hawkins' pioneering studies on the osmylation of C₆₀ and C₇₀.² In contrast to metal-bound fullerenes, ligand-bound fullerenes display enhanced kinetic stability.³ These species are of further interest with regards to the possible decomplexation of modified fullerenes. We are interested in the development of sulfur modified derivatives or *thiofullerenes* as precursors to more complex molecules or materials. We envision that thiofullerenes would allow attachment of a variety of electrophiles, to give fullerene thioethers, metal thiofullerides, and surface-bound species.

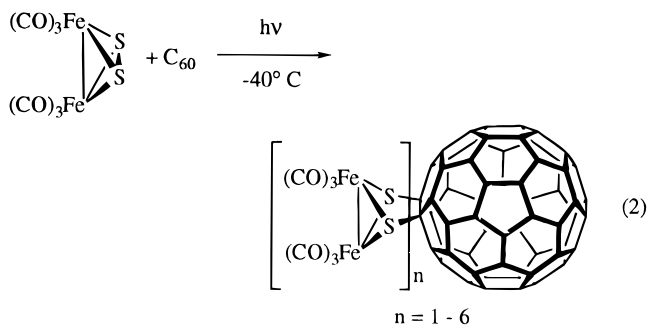
As a first step towards thiofullerenes, we prepared a series of metallothiofullerene derivatives. Elemental sulfur is known to cocrystallize with both C₆₀, C₇₀, and C₇₆⁴ but true thiofullerenes were unknown prior to this work.⁵ Our method involves the photoaddition of Fe₂S₂(CO)₆ to C₆₀ and C₇₀. The compound Fe₂S₂(CO)₆ was first synthesized by Hieber and Gruber⁶ and its structure was elucidated by Dahl's group.⁷ Over the past several years this compound has received much attention by virtue of the reactivity of the S–S bond,⁸ which in many ways behaves like an organic disulfide.⁹ Of particular interest is the fact that upon irradiation, Fe₂S₂(CO)₆ adds to alkenes (eq 1).¹⁰ In a preliminary report, we showed that this applies to C₆₀.¹¹



Since then we have completed the structural characterization of C₆₀S₂Fe₂(CO)₆ and extended the study to the use of Fe₂S₂(CO)_{6-x}L_x complexes as well as addition of the iron sulfides to C₇₀.

Results

Synthesis and Isolation of C₆₀[S₂Fe₂(CO)₆]_n. The project began with the observation that solutions of C₆₀ react with Fe₂S₂(CO)₆ upon UV irradiation to produce a series of soluble adducts. Reactions were typically conducted in toluene solution at –40 °C using a 10-fold excess of the iron reagent. Negative FAB-MS of crude reaction mixture revealed the presence of



C₆₀[S₂Fe₂(CO)₆]_n where n = 1–6 (eq 2). The product distribution could be monitored using HPLC on silica gel (Figure 1).

[⊗] Abstract published in *Advance ACS Abstracts*, November 1, 1996.

- (1) Fagan, P. J.; Calabrese, J. C.; Malone, B. *Acc. Chem. Res.* **1992**, *25*, 134. Balch, A. L.; Ginawalla, A. S.; Lee, J. W.; Noll, B. C.; Olmstead, M. M. *J. Am. Chem. Soc.* **1994**, *116*, 2227. Rasinkangas, M.; Pakkanen, T. T.; Pakkanen, T. A.; Ahlgren, M.; Rouvinen, J. *J. Am. Chem. Soc.* **1993**, *115*, 4901. Zhang, S.; Brown, T. L.; Du, Y.; Shapley, J. R. *J. Am. Chem. Soc.* **1993**, *115*, 6705.
- (2) Hawkins, J. M. *Acc. Chem. Res.* **1992**, *25*, 150. Hawkins, J. M.; Meyer, A.; Solow, M. A. *J. Am. Chem. Soc.* **1993**, *115*, 7499.
- (3) Yamage, S.; Yanagawa, M.; Nakamura, E. *J. Chem. Soc., Chem. Commun.* **1994**, 2093.
- (4) C₆₀S₈CS₂: Roth, G.; Adelman, P.; Knitter, R. *Mater. Lett.* **1993**, *16*, 357. C₇₀6S₈: Roth, G.; Adelman, P. *J. Phys. I* **1992**, *2*, 1541. C₇₆6S₈: Michel, R. H.; Kappes, M. M.; Adelman, P.; Roth, G. *Angew. Chem., Int. Ed. Engl.* **1994**, *33*, 1651; *Angew. Chem.* **1994**, *106*, 1742. Buravov, L. I.; D'yachenko, O. A.; Konovalikhin, S. V.; Kushch, N. D.; Lavrent'ev, I. P.; Spitsyna, N. G.; Shilov, G. V.; Yagubski, E. B. *Russ. Chem. Bull. (Engl. Transl.)* **1994**, *43*, 240.
- (5) Ohno, M.; Rojima, S.; Eguchi, S. *J. Chem. Soc., Chem. Commun.* **1995**, 565.
- (6) Hieber, W.; Gruber, J. *Z. Anorg. Allg. Chem.* **1958**, *296*, 91.
- (7) Wei, C. H.; Dahl, L. F. *Inorg. Chem.* **1965**, *4*, 1.

- (8) Seyferth, D.; Henderson, R. S.; Song, L.-C. *Organometallics* **1982**, *1*, 125. Seyferth, D.; Henderson, R. S. *J. Organomet. Chem.* **1981**, *218*, C34.
- (9) Seyferth, D.; Hoke, J. B.; Hofmann, P.; Schnellbach, M. *Organometallics* **1994**, *13*, 3452. Mathur, P.; Dash, A. K.; Hossain, M. M.; Umbarkar, S. B.; Satyanarayana, C. V. V.; Chen, Y.-S.; Rao, S. N.; Soriano, M. *Organometallics* **1996**, *15*, 1356.
- (10) Kramer, A.; Lingnau, R.; Lorenz, I.-P.; Mayer, H. A. *Chem. Ber.* **1990**, *123*, 1821. Kramer, A.; Lorenz, I.-P. *J. Organomet. Chem.* **1990**, *338*, 187. Müsselhauser, J.; Lorenz, I.-P.; Haug, K.; Hiller, W. *Z. Naturforsch.* **1985**, *40B*, 1064.
- (11) Westmeyer, M. D.; Galloway, C. P.; Rauchfuss, T. B. *Inorg. Chem.* **1994**, *33*, 4615.

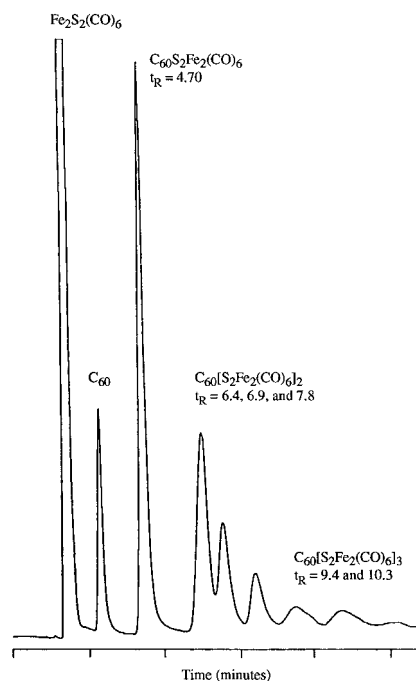


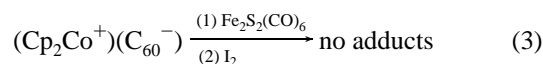
Figure 1. HPLC trace for the products of the photochemical reaction of $\text{Fe}_2\text{S}_2(\text{CO})_6$ and C_{60} (detector wavelength = 336 nm).

The HPLC analysis was calibrated with samples of mono-, di-, and triadducts which had been purified by preparative scale chromatography and checked by mass spectrometry. At short reaction times we observed the formation of the 1:1 adducts while prolonged reaction times resulted in complete conversion of the C_{60} and the formation of multiple addition compounds. Workup entailed filtration of the reaction mixture to remove the photodimer $\text{Fe}_4\text{S}_4(\text{CO})_{12}$.^{12,13} The filtrate consisted of unreacted $\text{Fe}_2\text{S}_2(\text{CO})_6$, $\text{C}_{60}[\text{S}_2\text{Fe}_2(\text{CO})_6]_n$, and unreacted C_{60} .

Preparative scale separations of $\text{C}_{60}[\text{S}_2\text{Fe}_2(\text{CO})_6]_n$ were accomplished by gel filtration on Bio-Beads SX-3 eluting with toluene. The purity and identity of the fractions were verified by HPLC and negative ion FAB-MS. The elution proceeds in the order of decreasing molecular size, the initial fraction consisting of small amounts of $\text{C}_{60}[\text{S}_2\text{Fe}_2(\text{CO})_6]_3$, followed by brown fractions of $\text{C}_{60}[\text{S}_2\text{Fe}_2(\text{CO})_6]_2$ and $\text{C}_{60}\text{S}_2\text{Fe}_2(\text{CO})_6$. A violet band of unreacted C_{60} was easily separated from the functionalized fullerenes. The optimized yield of $\text{C}_{60}\text{S}_2\text{Fe}_2(\text{CO})_6$ was ~50%, based on recovered C_{60} . The combined yield of the double and triple adducts was 20%. From a single reaction we could obtain 50 mg samples of $\text{C}_{60}\text{S}_2\text{Fe}_2(\text{CO})_6$ of >95% purity. The HPLC trace for the double addition product consisted of three peaks, suggesting the presence of at least three isomers. Eight isomers of $\text{C}_{60}[\text{S}_2\text{Fe}_2(\text{CO})_6]_2$ are possible.¹⁴ The FAB-MS of the $\text{C}_{60}[\text{S}_2\text{Fe}_2(\text{CO})_6]_3$ fraction confirmed the absence of $\text{C}_{60}\text{S}_2\text{Fe}_2(\text{CO})_6$ and $\text{C}_{60}[\text{S}_2\text{Fe}_2(\text{CO})_6]_2$.

Solutions of $\text{C}_{60}\text{S}_2\text{Fe}_2(\text{CO})_6$ are relatively stable even at higher temperatures. In refluxing toluene under nitrogen and carbon monoxide atmospheres, toluene solutions of $\text{C}_{60}\text{S}_2\text{Fe}_2(\text{CO})_6$ decomposes to give C_{60} and $\text{Fe}_2\text{S}_2(\text{CO})_6$ with a half-life of about 30 min. Under similar conditions $\text{C}_{60}[\text{S}_2\text{Fe}_2(\text{CO})_6]_2$ decays via a first-order process to first give $\text{C}_{60}\text{S}_2\text{Fe}_2(\text{CO})_6$ followed by C_{60} and $\text{Fe}_2\text{S}_2(\text{CO})_6$. Under these conditions, the diiron reagent is unstable with respect to the cubane cluster $\text{Fe}_4\text{S}_4(\text{CO})_{12}$. We attempted unsuccessfully to synthesize $\text{C}_{60}\text{S}_2\text{Fe}_2(\text{CO})_6$ via the

addition of C_{60}^- to $\text{S}_2\text{Fe}_2(\text{CO})_6$. A solution of C_{60} was treated with 1.1 equiv of Cp_2Co to precipitate the black $(\text{Cp}_2\text{Co})_x\text{C}_{60}$.¹⁵ Treatment of this suspension with $\text{Fe}_2\text{S}_2(\text{CO})_6$ followed by reoxidation with I_2 failed to give adducts (eq 3).



As for $\text{Fe}_2\text{S}_2(\text{CO})_6$, the IR spectrum of $\text{C}_{60}\text{S}_2\text{Fe}_2(\text{CO})_6$ consists of four ν_{CO} bands consistent with its C_{2v} symmetry. C_{60} itself exhibits no bands in this region. IR spectra of $\text{C}_{60}[\text{S}_2\text{Fe}_2(\text{CO})_6]_n$ are nearly identical for $n = 1-3$, indicating that there is little interaction between the $\text{S}_2\text{Fe}_2(\text{CO})_6$ sites. Optical spectroscopy proved to be the most sensitive measure of the degree of substitution at the fullerene cage. UV-vis maxima for the series $\text{C}_{60}[\text{S}_2\text{Fe}_2(\text{CO})_6]_n$ shift to shorter wavelength with increasing n , i.e. 336 ($n = 0$), 328 ($n = 1$), 322 ($n = 2$), and 318 nm ($n = 3$) (Figure 2).

The $^{13}\text{C}\{^1\text{H}\}$ NMR spectrum of $\text{C}_{60}\text{S}_2\text{Fe}_2(\text{CO})_6$ features 15 peaks for the cage, where 17 are expected. Four of these resonances should have half relative intensity arising from pairs of equivalent carbon atoms that lie on the two mirror planes of this C_{2v} molecule. On the basis of the observed signal intensities, at least two resonances are coincident, hence we can account for 16 of 17 possible signals. The chemical shifts (δ 135.8–154.1) are comparable to those of the nonfunctionalized carbon centers in $\text{C}_{60}\text{O}_2\text{OsO}_2(t\text{-Bupy})_2$ (δ 137–153).^{2,16} The resonances corresponding to the *ipso*-carbon and the carbonyl carbon atoms have not been assigned. The ^{13}C NMR resonance assigned to the *ipso*-carbon in osmylated fullerenes falls in the range δ 105–103.

Crystallographic Characterization of $\text{C}_{60}\text{S}_2\text{Fe}_2(\text{CO})_6$. The structure of $\text{C}_{60}\text{S}_2\text{Fe}_2(\text{CO})_6$ was confirmed by single-crystal X-ray diffraction (Figure 3). While the structure of the $\text{C}_{60}\text{S}_2\text{Fe}_2(\text{CO})_6$ refined well, we were unable to satisfactorily resolve the structures for the solvents of crystallization (toluene and pentane) which were also present in the unit cell. It is common for fullerenes to co-crystallize with solvent and the overall refinement was acceptable.¹⁷ The results confirm that the S–S bond in the starting $\text{Fe}_2\text{S}_2(\text{CO})_6$ ⁷ has been cleaved and that the sulfur ligands are attached to the C_{60} cage. The molecule is constrained to mirror symmetry although it also has idealized C_{2v} symmetry. The C(4)–C(5), Fe(1)–Fe(1a), C–S, and Fe–S bond distances are comparable to literature values for the cyclohexanedithiolate $\text{C}_6\text{H}_{12}\text{S}_2\text{Fe}_2(\text{CO})_6$ and the ethanedithiolate $\text{C}_2\text{H}_4\text{S}_2\text{Fe}_2(\text{CO})_6$.¹⁰ Compared to that in $\text{Fe}_2\text{S}_2(\text{CO})_6$, the S–Fe–S angle in the adduct has opened from 53.48 to 80.40°. Selected structural data are presented in Tables 3 and 4.

Synthesis of $\text{Fe}_2\text{S}_2(\text{CO})_{6-x}\text{L}_x$. We sought additional insight into the structure and reactivity of the $\text{C}_{60}\text{S}_2\text{Fe}_2(\text{CO})_6$ derivatives through studies on substituted analogs of the type $\text{C}_{60}\text{S}_2\text{Fe}_2(\text{CO})_5\text{L}$. We were unable to effect substitution of $\text{C}_{60}\text{S}_2\text{Fe}_2(\text{CO})_6$ by PPh_3 using Me_3NO ; instead, the amine oxide induced decomposition to C_{60} and unidentified iron-containing products.

A number of derivatives of $\text{Fe}_2\text{S}_2(\text{CO})_6$ were prepared by treatment of the hexacarbonyl with Me_3NO and a donor ligand.¹⁸

- (12) Nelson, L. L.; Lo, F. Y.; Rae, A. D.; Dahl, L. F. *J. Organomet. Chem.* **1982**, 225, 309.
 (13) Bogan, L. E., Jr.; Lesch, D. A.; Rauchfuss, T. B. *J. Organomet. Chem.* **1983**, 250, 429.
 (14) Hirsch, A.; Lamparth, I.; Karfunkel, H. R. *Angew. Chem., Int. Ed. Engl.* **1994**, 33, 437; *Angew. Chem.* **1994**, 106, 453.

- (15) Stinchcombe, J.; Pénicaud, A.; Bhyrappa, P.; Boyd, P. D. W.; Reed, C. A. *J. Am. Chem. Soc.* **1993**, 115, 5212. Bolskar, R. D.; Gallagher, S. H.; Armstrong, R. S.; Lay, P. A.; Reed, C. A. *Chem. Phys. Lett.* **1995**, 247, 57. Balch, A. L.; Lee, J. W.; Noll, B. C.; Olmstead, M. M. In *Fullerenes: Recent Advances in the Chemistry and Physics of Fullerenes and Related Materials*; Kadish, K. M., Ruoff, R. J., Eds.; The Electrochemical Society: Pennington, NJ, 1996; Vol. 94-26, p 1231.
 (16) For C_{60}O , the shifts for the unfunctionalized carbon atoms occur at δ 140–146 (Creagan, K. M.; Robbins, J. L.; Robbins, W. K.; Millar, J. M.; Sherwood, R. D.; Tindall, P. J.; Cox, D. M.; Smith, A. B., III; McCauley, J. P.; Jones, D. R.; Gallagher, R. T. *J. Am. Chem. Soc.* **1992**, 114, 1103).
 (17) Balch, A. L.; Lee, J. W.; Noll, B. C.; Olmstead, M. M. *Inorg. Chem.* **1994**, 33, 5238.

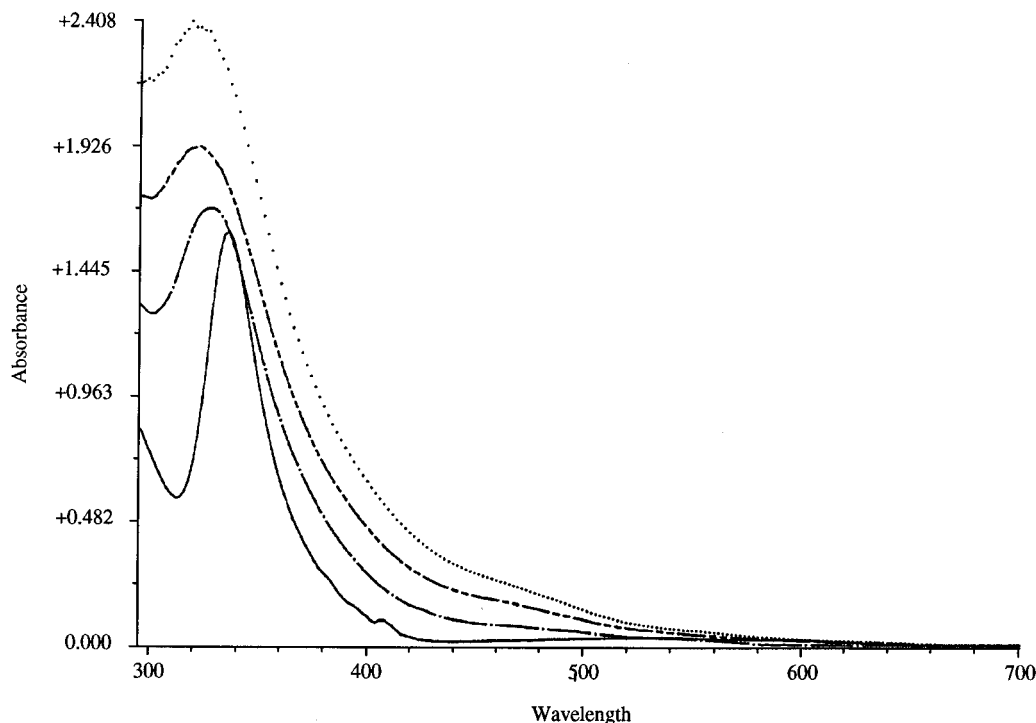


Figure 2. UV-vis spectra of $C_{60}[S_2Fe_2(CO)_6]_n$ for $n = 0$ (solid line), $n = 1$ (---), $n = 2$ (-·-·-), and $n = 3$ (···).

Table 1. Spectroscopic and Electrochemical Data for Fullerene Derivatives

compound	ν_{CO} (cm^{-1}) ^a	λ_{max} (nm) ^b	$E_{1/2}$ (mV) vs Ag/AgCl ^c
C_{60}		336	-474, -854, -1306, -1767
$C_{60}S_2Fe_2(CO)_6$	2076, 2040, 2011, 2001	328	-450, -831, -1281, -1762
$C_{60}[S_2Fe_2(CO)_6]_2$	2076, 2041, 2012, 2002	322	-446, -797, -1300, -1795
$C_{60}[S_2Fe_2(CO)_6]_3$	2044, 2041, 2012, 2002	318	-413, -834, -1292, -1750
$C_{60}S_2Fe_2(CO)_5(PPh_3)$	2045, 1995, 1980, 1943	332	-476, -834, -1276, -1759
$C_{60}[S_2Fe_2(CO)_5(PPh_3)]_2$	2044, 1985, 1970, 1942	330	
C_{70}		334	-488, -858, -1253, -1660
$C_{70}S_2Fe_2(CO)_6$	2076, 2040, 2011, 2001		-495, -890, -1256, -1644
$C_{70}[S_2Fe_2(CO)_6]_2$	2076, 2040, 2011, 2001	312	
$C_{70}[S_2Fe_2(CO)_6]_3$	2075, 2041, 2012, 2001	316	

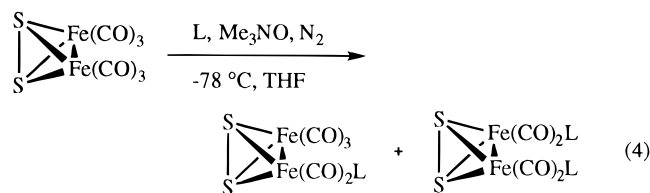
^a CS_2 solutions. ^b Toluene solutions in the 300–700 nm range. ^c 0.1 mM 1,2-dichlorobenzene solution of *n*-Bu₄NPF₆.

Table 2. Spectroscopic Data for $Fe_2S_2(CO)_{6-x}L_x$ Reagents

compound	ν_{CO} (cm^{-1}) ^a	λ (nm) ^b	δ_{CO} (ppm) ^c	δ_P (ppm) ^d
$Fe_2S_2(CO)_6$	2080, 2039, 2001	338	208.6	
$Fe_2S_2(CO)_5(PPh_3)$	2054, 1994, 1983	364	216.4–216.3, 210.1	60.82
$Fe_2(SMe)_2(CO)_6$	2069, 2032, 1990, 1986	334	209.4	
$Fe_2(SMe)_2(CO)_5(PPh_3)$	2042, 1983, 1973, 1962	372	216.4, 210.8	61.69, 57.07 ^e

^a Hexanes solution. ^b Toluene solution in 300–700 nm range. ^c $^{13}C\{^1H\}$ NMR in benzene-*d*₆. ^d $^{31}P\{^1H\}$ NMR in benzene-*d*₆. ^e Minor isomer (*e, e*).

In this way we obtained reasonable yields of $Fe_2S_2(CO)_5L$, where $L = PPh_3, P(4-C_6H_4OMe)_3, CN^tBu,$ and CN^iPh (eq 4).



We were unable to prepare adducts with $(Ph_2P)_2CH_2$. The PPh_3 adduct, which had been prepared previously by alternative methods,¹⁹ proved to be most stable and we focused our efforts

(18) Luh, T.-Y. *Coord. Chem. Rev.* **1984**, *60*, 255. Shvo, Y.; Hazum, E. *J. Chem. Soc., Chem. Commun.* **1974**, 336; **1975**, 829.

(19) Rossetti, R.; Gervasio, G.; Stanghellini, P. L. *Inorg. Chim. Acta* **1979**, *35*, 73.

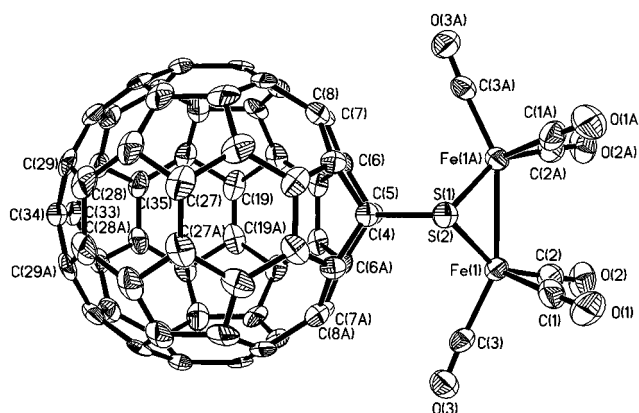


Figure 3. Structure of $C_{60}S_2Fe_2(CO)_6$ with thermal ellipsoids set at the 50% probability level.

on its use. The $^{13}C\{^1H\}$ NMR spectrum of $Fe_2S_2(CO)_5(PPh_3)$ shows two signals: a multiplet at δ 216.4–216.3 and a singlet

Table 3. Crystal Data and Structural Refinement for Parameters $C_{60}S_2Fe_2(CO)_6$

empirical formula: $C_{66}Fe_2O_6S_2 \cdot C_{4.78}H_{6.33}$
fw = 1128.25
temperature: 198(2) K
wavelength: 0.710 73 Å
crystal system: trigonal
space group: $R\bar{3}m$
unit cell dimens: $a = 27.284(8)$ Å, $b = 27.284(8)$ Å, $c = 14.675(3)$ Å, $\alpha = 90^\circ$, $\beta = 90^\circ$, $\gamma = 120^\circ$
$V = 9461(4)$ Å ³
$Z = 9$
$d(\text{calcd}) = 1.782$ mg/m ³
abs coeff: 0.862 mm ⁻¹
crystal size: 0.26 × 0.24 × 0.22 mm
θ range for data collection: 1.49–23.98°
index ranges: $-31 \leq h \leq 0$, $-27 \leq k \leq 31$, $-16 \leq l \leq 0$
collec method: ω - θ scan profiles
no. of reflns: 5273 [$R(\text{int}) = 0.0489$] ^a
no. of indep reflns: 1845 [1642 obs, $I > 2\sigma(I)$]
refinement method (shift/err = -0.138): full-matrix least-squares on F^2
data/restraints/parameters: 1845/15/392
goodness-of-fit on F^2 : 1.037
final R indices (obs data): $R_1 = 0.0567$, $wR_2 = 0.1479$ ^b
R indices (all data): $R_1 = 0.0669$, $wR_2 = 0.1568$
absolute structural parameter: 0.08(4)
largest diff peak and hole: 1.899 and -0.781 e ⁻ Å ⁻³
^a $R(\text{int}) = \sum F_o^2 - F_c^2(\text{mean}) / \sum [F_o^2 - F_c^2]$; ^b $wR_2 = [\sum w(F_o^2 - F_c^2)^2] / \sum [w(F_o^2)^2]$, where $w = 1/[\sigma^2(F_o^2) + (0.0109P)^2 + 7.5500P]$, where $P = (F_o^2 - 2F_c^2)/3$.

Table 4. Selected Bond Lengths (Å) and Bond Angles (deg) for $C_{60}S_2Fe_2(CO)_6$

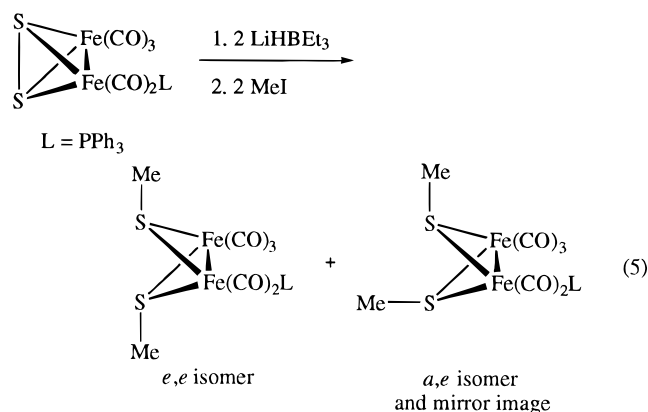
Bond Lengths (Å)			
Fe(1)–Fe(1A)	2.510(2)	C(14)–C(23)	1.434(9)
Fe(1)–S(1)	2.227(2)	C(15)–C(16)	1.385(7)
Fe(1)–S(2)	2.237(2)	C(16)–C(17)	1.438(8)
Fe(1)–C(1)	1.822(7)	C(16)–C(21)	1.456(9)
Fe(1)–C(2)	1.819(7)	C(17)–C(18)	1.381(9)
Fe(1)–C(3)	1.811(6)	C(17)–C(19)	1.436(9)
S(1)–S(2)	2.881(3)	C(18)–C(18A)	1.448(13)
S(1)–C(4)	1.897(8)	C(19)–C(19A)	1.375(2)
S(2)–C(5)	1.869(8)	C(19)–C(20)	1.485(9)
C(1)–O(1)	1.121(8)	C(20)–C(21)	1.436(9)
C(2)–O(2)	1.116(8)	C(21)–C(22)	1.401(8)
C(3)–O(3)	1.100(8)	C(22)–C(23)	1.417(8)
C(4)–C(5)	1.537(10)	C(22)–C(31)	1.434(9)
C(4)–C(9)	1.514(7)	C(23)–C(24)	1.434(9)
C(5)–C(6)	1.549(8)	C(24)–C(25)	1.386(9)
C(6)–C(7)	1.365(7)	C(24)–C(30)	1.454(8)
C(6)–C(18)	1.418(7)	C(25)–C(26)	1.431(11)
C(7)–C(8)	1.484(7)	C(26)–C(27)	1.468(10)
C(7)–C(15)	1.414(8)	C(26)–C(28)	1.406(10)
C(8)–C(9)	1.382(9)	C(27)–C(27A)	1.391(14)
C(8)–C(13)	1.441(8)	C(28)–C(28A)	1.426(2)
C(9)–C(10)	1.441(8)	C(28)–C(29)	1.424(10)
C(10)–C(10A)	1.439(13)	C(29)–C(30)	1.382(10)
C(10)–C(11)	1.434(9)	C(29)–C(34)	1.436(8)
C(11)–C(27)	1.418(10)	C(30)–C(31)	1.425(8)
C(11)–C(12)	1.434(10)	C(31)–C(32)	1.419(9)
C(12)–C(13)	1.415(9)	C(32)–C(33)	1.438(9)
C(12)–C(25)	1.410(10)	C(32)–C(35)	1.456(8)
C(13)–C(14)	1.425(9)	C(33)–C(34)	1.440(13)
C(14)–C(15)	1.447(7)	C(35)–C(35A)	1.434(2)
Bond Angles (deg)			
S(1)–Fe(1)–S(2)	80.4(7)	S(1)–C(4)–C(9)	106.0(4)
S(1)–Fe(1)–C(1)	91.1(2)	C(5)–C(4)–C(9)	116.8(4)
S(1)–Fe(1)–C(2)	152.7(2)	S(2)–C(4)–C(5)	112.1(5)
S(1)–Fe(1)–C(3)	109.0(2)	S(2)–C(5)–C(6)	107.7(4)
Fe(1A)–Fe(1)–S(1)	55.69(4)	C(4)–C(5)–C(6)	114.7(4)
Fe(1)–S(1)–C(4)	104.8(2)	C(4)–C(9)–C(8)	122.6(5)
Fe(1)–S(1)–Fe(1A)	68.62(7)	C(7)–C(8)–C(9)	121.0(5)
Fe(1)–S(2)–C(5)	104.4(2)	C(6)–C(7)–C(8)	119.5(5)
Fe(1)–S(2)–Fe(1A)	68.25(7)	C(5)–C(6)–C(7)	123.5(5)
S(1)–C(4)–C(5)	109.8(5)		

at δ 210.1. We assign these CO signals to $Fe(CO)_2(PPh_3)$ and $Fe(CO)_3$, respectively. A ¹³C NMR resonance was observed

at δ 218.4 for $Fe_2S_2(CO)_4(PPh_3)_2$, a compound that was obtained as a byproduct in the synthesis of $Fe_2S_2(CO)_5(PPh_3)$. The ³¹P-¹H NMR spectra for $Fe_2S_2(CO)_5(PPh_3)$ and $Fe_2S_2(CO)_4(PPh_3)_2$ consist of single resonances at δ 60.81 and δ 58.19, respectively.

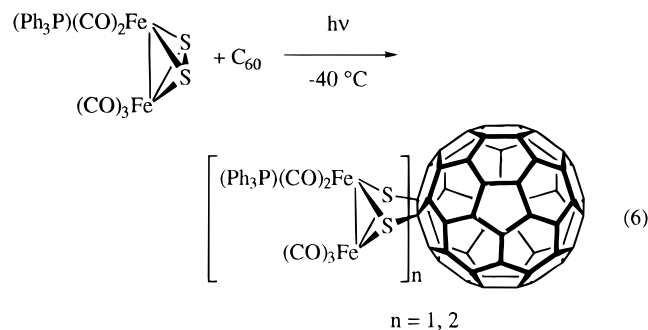
$Fe_2S_2(CO)_5(PPh_3)$ is thermally more stable than $Fe_2S_2(CO)_6$ since the unsubstituted compound decomposes at temperatures above 40 °C and readily photodimerizes. In contrast, solutions of $Fe_2S_2(CO)_5(PPh_3)$ are stable at 100 °C for days and only slowly decompose photochemically. Decomposition of $Fe_2S_2(CO)_5(PPh_3)$, as monitored by ³¹P{¹H} NMR spectroscopy, produces $SPPH_3$.

The reactivity of the S–S bond in $Fe_2S_2(CO)_6(PPh_3)$ was probed by chemical reduction followed by alkylation. Reduction using 2 equiv of $LiBHET_3$ gave deep green solutions, as seen for the parent hexacarbonyl.²⁰ Addition of iodomethane to these solutions gave good yields of $(MeS)_2Fe_2(CO)_5(PPh_3)$. ¹H and ³¹P{¹H} NMR spectroscopies established the presence of two isomers which differ in terms of the relative orientations of the methyl groups. The unsymmetrical derivative must be assigned as the axial–equatorial isomer (*a,e*) while the symmetrical isomer is almost certainly diequatorial (*e,e*) (eq 5). $(MeS)_2Fe_2-$



$(CO)_6$ exists as *a,e* and *e,e* isomers in a 2.4:1 ratio while for $(MeS)_2Fe_2(CO)_5(PPh_3)$ the isomer ratio is 15:1. The isomer ratio indicates that the PPh_3 ligand destabilizes the equatorial methyl group relative to the axial orientation.²¹

Synthesis and Characterization of $C_{60}S_2Fe_2(CO)_5(PPh_3)$. UV irradiation of solutions of C_{60} and $Fe_2S_2(CO)_{6-x}(PPh_3)_x$ resulted in product formation only for the case where $x = 1$ (eq 6).²² Unreacted $Fe_2S_2(CO)_5(PPh_3)$ and $SPPH_3$, a byproduct



(20) Seyferth, D.; Kiwan, A. M. *J. Organomet. Chem.* **1985**, *281*, 111. Weatherill, T. D.; Rauchfuss, T. B.; Scott, R. A. *Inorg. Chem.* **1986**, *25*, 1466.

(21) We also prepared $(MeS)_2Fe_2(CO)_4(PPh_3)_2$; here the *a,e,e,e* ratio is 2.4:1, as seen for the hexacarbonyl.

(22) Photoaddition to C_{60} was not observed for $Fe_2S_2(CO)_5(CNBu)_1$, $Fe_2S_2(CO)_5\{P(4-C_6H_4OMe)_3\}$, or $Fe_2S_2(CO)_4(PPh_3)_2$ although in these cases we have independently verified that the persulfide bond is reactive toward reduction followed by methylation.

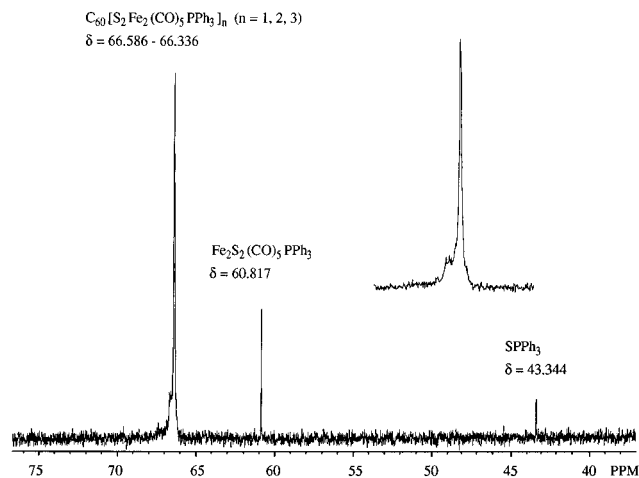


Figure 4. 161 MHz $^{31}\text{P}\{^1\text{H}\}$ NMR spectrum of $\text{C}_{60}[\text{S}_2\text{Fe}_2(\text{CO})_5(\text{PPh}_3)]_n$ in benzene- d_6 . Inset: Expansion of the low-field signal.

of the reaction, were removed by washing the reaction mixture with acetone, leaving a mixture of fullerenes which was then purified as for the hexacarbonyl derivatives. Positive FAB-MS of the crude reaction mixture indicated the presence of $\text{C}_{60}[\text{S}_2\text{Fe}_2(\text{CO})_5(\text{PPh}_3)]_n$ where $n = 1-3$. Figure 4 shows a $^{31}\text{P}\{^1\text{H}\}$ NMR spectrum of a representative reaction mixture. Our syntheses typically produced $\text{C}_{60}\text{S}_2\text{Fe}_2(\text{CO})_5(\text{PPh}_3)$ and $\text{C}_{60}[\text{S}_2\text{Fe}_2(\text{CO})_5(\text{PPh}_3)]_2$ in 34 and 43% yields, respectively. In contrast to the synthesis of $\text{C}_{60}\text{S}_2\text{Fe}_2(\text{CO})_6$, we observed only trace amounts of higher adducts. Photodimerization of $\text{Fe}_2\text{S}_2(\text{CO})_5(\text{PPh}_3)$ was not detected.

Toluene solutions of $\text{C}_{60}\text{S}_2\text{Fe}_2(\text{CO})_5(\text{PPh}_3)$, while quite stable, are demonstrably more labile than the hexacarbonyl derivatives. At ambient temperatures, toluene solutions of $\text{C}_{60}\text{S}_2\text{Fe}_2(\text{CO})_5(\text{PPh}_3)$ decompose with a $t_{1/2}$ of 9.4 days compared to $\text{C}_{60}\text{S}_2\text{Fe}_2(\text{CO})_6$, which is stable for weeks in solution. The $^{31}\text{P}\{^1\text{H}\}$ NMR spectrum of $\text{C}_{60}\text{S}_2\text{Fe}_2(\text{CO})_5(\text{PPh}_3)$ consists of a single peak at δ 66.2, vs δ 60.8 for starting $\text{Fe}_2\text{S}_2(\text{CO})_5(\text{PPh}_3)$. The $^{31}\text{P}\{^1\text{H}\}$ NMR spectrum of $\text{C}_{60}[\text{S}_2\text{Fe}_2(\text{CO})_5(\text{PPh}_3)]_2$ shows a multiplet in the range of δ 66.7–66.1, indicative of the presence of multiple isomers.

The IR spectrum of $\text{C}_{60}\text{S}_2\text{Fe}_2(\text{CO})_5(\text{PPh}_3)$ consists of four ν_{CO} bands which are only slightly shifted from that of the starting $\text{Fe}_2\text{S}_2(\text{CO})_5(\text{PPh}_3)$. The higher energy ν_{CO} band for $\text{Fe}_2\text{S}_2(\text{CO})_5(\text{PPh}_3)$ at 2054 cm^{-1} shifts to 2045 cm^{-1} for $\text{C}_{60}\text{S}_2\text{Fe}_2(\text{CO})_5(\text{PPh}_3)$. The optical spectrum showed a maximum at 332 nm vs 336 nm for C_{60} and 328 nm for $\text{C}_{60}\text{S}_2\text{Fe}_2(\text{CO})_6$.

Electrochemical Studies of $\text{C}_{60}\text{S}_2\text{Fe}_2(\text{CO})_5\text{L}$ Compounds. The redox properties of the modified fullerenes were evaluated by cyclic voltammetry on 1,2-dichlorobenzene solutions (Table 1).²³ We confirmed that neither $\text{Fe}_2\text{S}_2(\text{CO})_6$ nor $\text{Fe}_2\text{S}_2(\text{CO})_5(\text{PPh}_3)$ is electroactive over the region of interest. We observed four reductions for $\text{C}_{60}\text{S}_2\text{Fe}_2(\text{CO})_6$ at -450 , -831 , -1281 , and -1782 mV vs Ag/AgCl . These couples appear reversible based on the $i_{\text{cp}}/i_{\text{ap}}$ ratios. In comparison to C_{60} itself, the first couple is shifted cathodically by 25 mV.²⁴ The first reduction potentials for the higher adducts ($n = 2, 3$) are also shifted. In contrast, the first reduction wave of $\text{C}_{60}\text{S}_2\text{Fe}_2(\text{CO})_5(\text{PPh}_3)$ is indistinguishable from that of C_{60} itself.

Synthesis of $\text{C}_{70}[\text{S}_2\text{Fe}_2(\text{CO})_6]_n$. UV irradiation of toluene solutions of $\text{Fe}_2\text{S}_2(\text{CO})_6$ and C_{70} afforded soluble products whose negative FAB-MS indicated the presence of $\text{C}_{70}[\text{S}_2\text{Fe}_2(\text{CO})_6]_n$ where $n = 1-4$ (eq 7). Figure 5 shows the HPLC trace for a

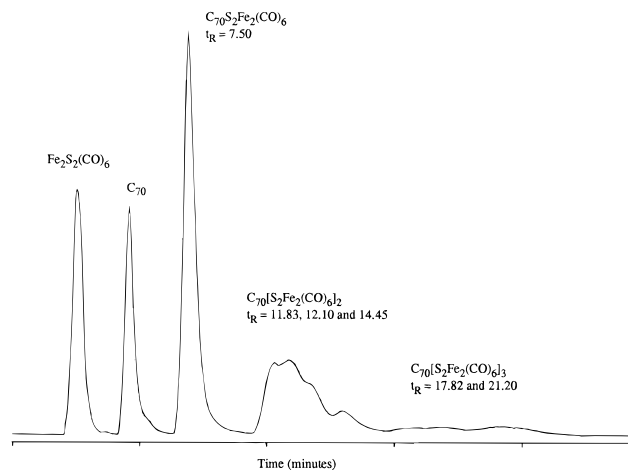
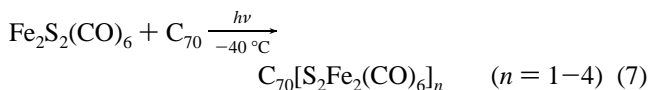


Figure 5. HPLC trace for the products of the photochemical reaction of $\text{Fe}_2\text{S}_2(\text{CO})_6$ and C_{70} after irradiation (detector wavelength = 334 nm).

representative reaction mixture. The reaction products were purified using the method developed for $\text{C}_{60}[\text{S}_2\text{Fe}_2(\text{CO})_6]_n$. Four bands were obtained: $\text{C}_{70}[\text{S}_2\text{Fe}_2(\text{CO})_6]_n$ ($n = 3, 4$), followed by $\text{C}_{70}[\text{S}_2\text{Fe}_2(\text{CO})_6]_2$, $\text{C}_{70}\text{S}_2\text{Fe}_2(\text{CO})_6$, and finally unreacted C_{70} . HPLC showed a single peak for $\text{C}_{70}\text{S}_2\text{Fe}_2(\text{CO})_6$, indicating a single isomer. We observed four peaks for $\text{C}_{70}[\text{S}_2\text{Fe}_2(\text{CO})_6]_2$ and three peaks for $\text{C}_{70}[\text{S}_2\text{Fe}_2(\text{CO})_6]_3$.



The IR spectrum of $\text{C}_{70}\text{S}_2\text{Fe}_2(\text{CO})_6$ is almost indistinguishable from that of $\text{Fe}_2\text{S}_2(\text{CO})_6$. Analogous to the case for the C_{60} adducts, the $\text{C}_{70}[\text{S}_2\text{Fe}_2(\text{CO})_6]_n$ adducts ($n = 1-3$) have IR spectra nearly identical to that of $\text{C}_{70}\text{S}_2\text{Fe}_2(\text{CO})_6$. The optical spectrum of $\text{C}_{70}\text{S}_2\text{Fe}_2(\text{CO})_6$ consists of a featureless sloping band in contrast to C_{70} (Table 1).

The $^{13}\text{C}\{^1\text{H}\}$ NMR spectrum of $\text{C}_{70}\text{S}_2\text{Fe}_2(\text{CO})_6$ provides some insight into the stereochemistry of this adduct. This spectrum consists of 37 resonances (Figure 6). This observation alone suggests that the adduct consists of a single isomer. Figure 7 shows the four possible isomers for 1:1 adducts together with their point group symmetry and the number of expected ^{13}C NMR C_{70} resonances. Addition across the 6,6 ring fusions can lead to adducts of C_s (two isomers), C_1 , and C_{2v} symmetry. These correspond to additions across the 1-2, 3-3, 4-5, and the 5-5 bonds, respectively. On the basis of the $^{13}\text{C}\{^1\text{H}\}$ NMR spectrum, the product has C_s symmetry. This is consistent with addition across the 1-2 bond, the part of the cage with the greatest curvature.^{24,25}

Cyclic voltammetric studies reveal that the redox properties of $\text{C}_{70}\text{S}_2\text{Fe}_2(\text{CO})_6$ and C_{70} are similar. The metallothiofullerene species displays reversible reductions at -495 , -890 , -1256 , and -1644 mV and an irreversible reduction at -1156 mV vs Ag/AgCl (Table 1).

UV irradiation of an equimolar solution of C_{60} and C_{70} with $\text{Fe}_2\text{S}_2(\text{CO})_6$ resulted in consumption of the two fullerenes at the same rate (Figure 8). This suggests that the rate-determining step in the reaction involves photoactivation of the Fe_2 reagent to give $\text{Fe}_2(\text{S})_2(\text{CO})_6^*$ which, in a rapid subsequent step, reacts with the fullerenes.

Discussion

It is known that C_{60} or C_{70} can be recrystallized intact from molten sulfur as well from CS_2 solutions of sulfur.⁴ The

(23) Suzuki, T.; Maruyama, Y.; Akasaka, T.; Ando, W. *J. Am. Chem. Soc.* **1994**, *116*, 1359.

(24) Boudon, C.; Gisselbrecht, J.-P.; Gross, M.; Isaacs, L.; Anderson, H. L.; Faust, R.; Diederich, F. *Helv. Chim. Acta* **1995**, *78*, 1324.

(25) Hawkins, J. M.; Meyer, A.; Solow, M. A. *J. Am. Chem. Soc.* **1993**, *115*, 7499.

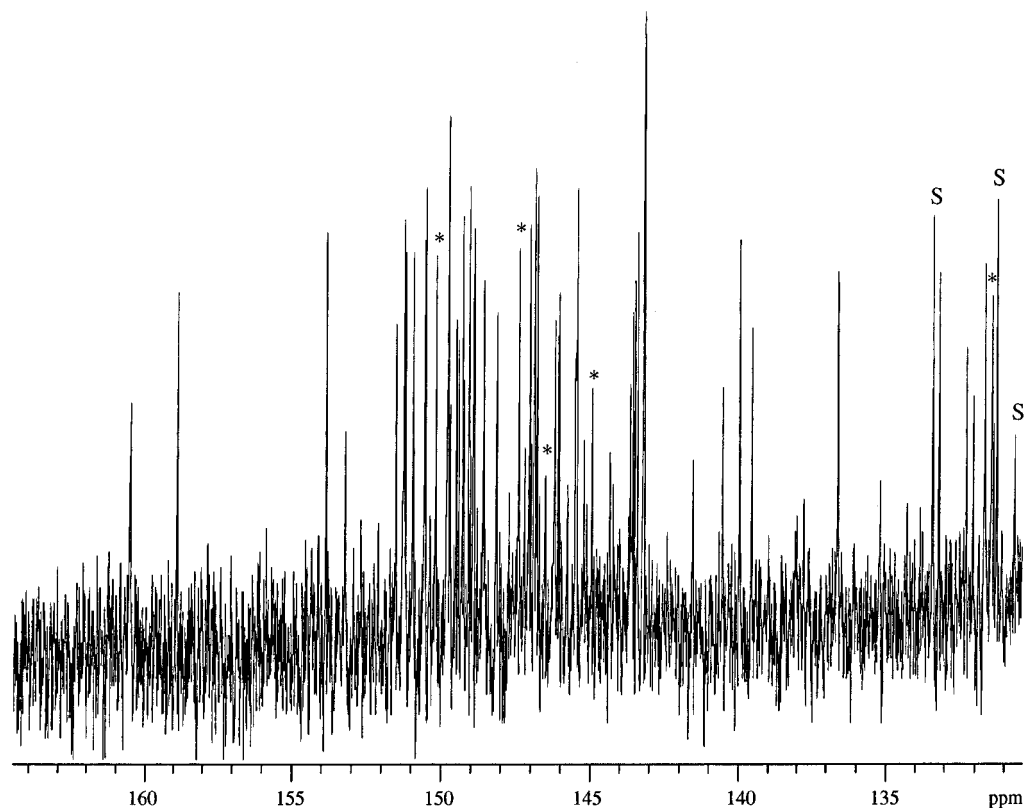


Figure 6. 125 MHz $^{13}\text{C}\{^1\text{H}\}$ NMR spectrum of $\text{C}_{70}\text{S}_2\text{Fe}_2(\text{CO})_6$ in 1:1 CS_2 and benzene- d_6 .

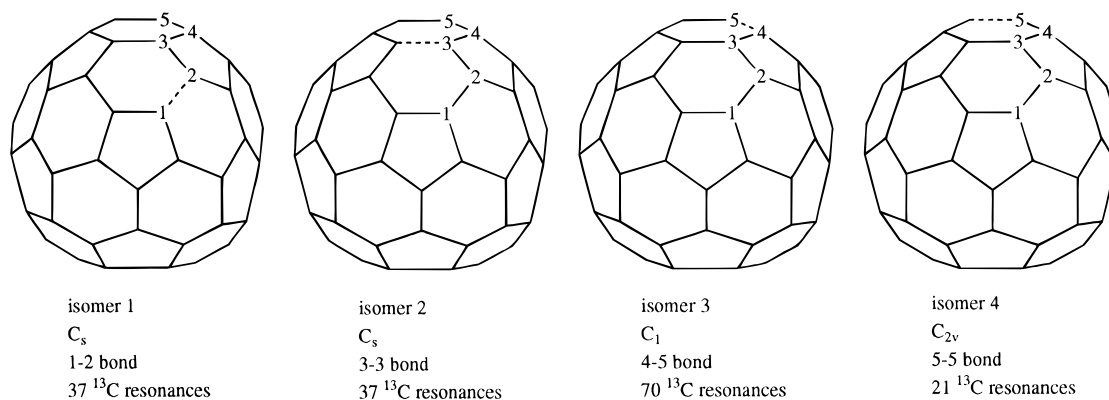
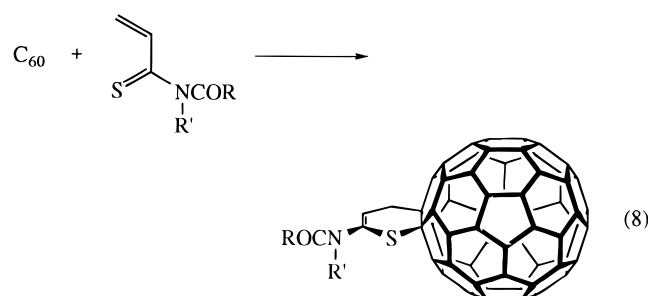


Figure 7. Four possible isomers of $\text{C}_{70}\text{S}_2\text{Fe}_2(\text{CO})_6$. C_{70} is viewed down the C_5 axis.

resulting solids, having the formulas $\text{C}_{60}(\text{S}_8)(\text{CS}_2)$, $\text{C}_{70}(\text{S}_8)_6$, and $\text{C}_{76}(\text{S}_8)_6$, are composed of isolated fullerene cages and S_8 rings. The interactions between the fullerene cages and S_8 rings in these solids are weak and no covalent C–S bonds are observed. Subsequent to our work, Eguchi *et al.* reported the 1,3-dipolar cycloaddition reaction of *N*-acylthioacrylamide with C_{60} to produce a dihydrothiopyran-fused [60]fullerene (eq 8).⁵



This project produced the double-cage species $\text{C}_{60}\text{S}_2\text{Fe}_2(\text{CO})_6$ in good yield by UV irradiation of toluene solutions of C_{60} and $\text{Fe}_2\text{S}_2(\text{CO})_6$. The photoaddition of $\text{Fe}_2\text{S}_2(\text{CO})_6$ to double bonds¹⁰

is thought to proceed via the homolytic cleavage of the S–S bond to give the (bis- μ -sulfide) $\text{Fe}_2(\text{S})_2(\text{CO})_6^*$. This species can react in three ways, it can add to a fullerene to produce adducts, it can react with $\text{Fe}_2\text{S}_2(\text{CO})_6$ to produce $\text{Fe}_4\text{S}_4(\text{CO})_{12}$, or it can revert to $\text{Fe}_2\text{S}_2(\text{CO})_6$. The resulting $\text{C}_{60}\text{S}_2\text{Fe}_2(\text{CO})_6$ adducts are metastable, indicated by their conversion to C_{60} and $\text{Fe}_2\text{S}_2(\text{CO})_6$ upon heating to 100 °C. The thermal decomposition of $\text{C}_{60}\text{S}_2\text{Fe}_2(\text{CO})_5(\text{PPh}_3)$ proceeds more cleanly and under milder conditions to give C_{60} and $\text{Fe}_2\text{S}_2(\text{CO})_5(\text{PPh}_3)$. Evidence supporting the thermodynamic instability of $\text{C}_{60}\text{S}_2\text{Fe}_2(\text{CO})_6$ is provided by our inability to prepare these adducts by thermal routes including reactions of C_{60}^- with $\text{Fe}_2\text{S}_2(\text{CO})_6$ and $\text{Fe}_2(\text{S})_2(\text{CO})_6^{2-}$ with C_{60} . Carbanions are known to cleave the S–S bond in this diiron reagent to give $\text{Fe}_2(\text{SR})(\text{S}^-)(\text{CO})_6$ which are susceptible to a second alkylation by electrophilic reagents ($\text{R}'\text{X}$) to give $\text{Fe}_2(\text{CO})_6(\text{SR})(\text{SR}')$.⁹

The photoaddition reaction is strongly affected upon replacement of CO by PPh_3 . The use of $\text{Fe}_2\text{S}_2(\text{CO})_5(\text{PPh}_3)$ leads mainly 1:1 and 2:1 adducts whereas up to 6 equiv of $\text{Fe}_2\text{S}_2(\text{CO})_6$ could be added. Additionally, the rate of the photoaddition process was slower for $\text{Fe}_2\text{S}_2(\text{CO})_5(\text{PPh}_3)$. It thus appears that the

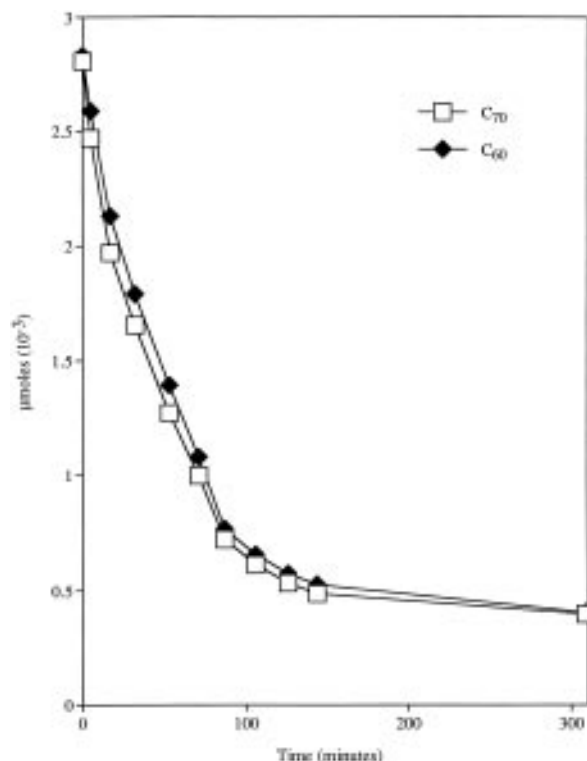


Figure 8. Time course for the photochemical reaction of $\text{Fe}_2\text{S}_2(\text{CO})_6$ and an equimolar mixture of C_{60} and C_{70} (detector wavelength = 336 nm).

degree and rates of additions are strongly influenced by steric factors. By virtue of the unsymmetrical nature of $\text{Fe}_2\text{S}_2(\text{CO})_5(\text{PPh}_3)$, several isomers of the 2:1 adduct are possible. This complexity is evident from the $^{31}\text{P}\{^1\text{H}\}$ NMR spectrum for $\text{C}_{60}[\text{S}_2\text{Fe}_2(\text{CO})_5(\text{PPh}_3)]_2$.

The photoaddition of $\text{Fe}_2\text{S}_2(\text{CO})_6$ to C_{70} proceeded similarly to the C_{60} reaction, leading to $\text{C}_{70}[\text{S}_2\text{Fe}_2(\text{CO})_6]_n$ where $n = 1-4$. HPLC and ^{13}C NMR measurements indicate that the 1:1 adduct exists as a single isomer, where four are possible.²⁵ Balch *et al.* described the fact that, in $\text{C}_{70}[\text{IrCl}(\text{CO})(\text{PPh}_3)_2]$, the iridium atom is bound to C(1) and C(2), the 6-6 bond of greatest curvature.²⁶ Diederich made a similar observation in his study of the cyclopropanation of C_{70} .^{27,28} UV irradiation of a solution containing $\text{Fe}_2\text{S}_2(\text{CO})_6$ and an equimolar mixture of C_{60} and C_{70} revealed that the rates of consumption of C_{60} and C_{70} were identical (Figure 8). This result indicates that the rate-limiting step in the addition process is generation of $\text{Fe}_2(\text{S})_2(\text{CO})_6^*$, which in a fast subsequent step binds the fullerenes.

Experimental Section

General Procedures. All reactions were carried out under a nitrogen atmosphere involving standard Schlenk techniques. C_{60} (99.8%, Southern Chemical Group or SES Research), C_{70} (98%, Southern Chemical Group), PPh_3 (Kodak), 1.0 M LiEt_3BH in THF (Super-Hydride, Aldrich), Bio-Beads SX-3 (Bio-Rad), cobaltocene (Aldrich), iodine (Fisher Scientific), iodomethane (Aldrich), and Paratone oil (Exxon) were used without further purification. $\text{Me}_3\text{N}\cdot\text{H}_2\text{O}$ (Aldrich) was dehydrated and purified by triple vacuum sublimation. $\text{Fe}_2\text{S}_2(\text{CO})_6$ was prepared by a recently improved method.²⁹ Toluene and tetrahy-

drofuran (THF) were distilled from sodium benzophenone ketyl. 1,2-Dichlorobenzene was distilled over sodium at reduced pressure prior to use.

Reactions were monitored by HPLC at $\lambda = 336$ nm with hexanes as the solvent (Varian 2510 HPLC pump, 2550 UV detector, and Baxter BASSI5 SG Silica column). Elution rates were 1 mL/min for the hexacarbonyl derivatives and 2 mL/min for the triphenylphosphine derivatives. Irradiations were performed with a Spectronic Black Light Lamp ($\lambda = 365$ nm) Spectroline Model MB-100. Infrared spectra were obtained with a Mattson Galaxy Series FT-IR 3000 using a NaCl solution cell. Optical spectra were obtained with a Hewlett-Packard 8452A diode array spectrophotometer, the peak maxima are separated in nm. ^1H and $^{13}\text{C}\{^1\text{H}\}$ NMR spectra were recorded on GE 500 MHz FT-NMR and U-400 Varian FT-NMR spectrometers. Chemical shifts are reported in δ units versus TMS. $^{31}\text{P}\{^1\text{H}\}$ NMR spectra were recorded on a U-400 Varian FT-NMR spectrometer with chemical shifts referenced to 85% H_3PO_4 . Mass spectra were obtained by the University of Illinois Mass Spectroscopy Laboratory. Microanalyses were performed by the School of Chemical Sciences Microanalytical Laboratory.

Cyclic voltammograms were recorded on a Bioanalytical System BAS-100 electrochemical analyzer using platinum as the working electrode. All measurements were referenced to Ag/AgCl . Measurements were performed at ambient temperatures under a nitrogen atmosphere on a 0.1 mM 1,2-dichlorobenzene solutions of $(n\text{-Bu})_4\text{NPF}_6$. Fullerene concentrations ranged from 0.25 to 0.30 mM. *iR* compensation was employed with each measurement.

$\text{C}_{60}[\text{S}_2\text{Fe}_2(\text{CO})_6]_n$. A 250-mL Schlenk flask was charged with 300 mg (0.417 mmol) of C_{60} and 100 mL of toluene. The violet solution was then cooled to -40 °C (acetonitrile/ CO_2) followed by the addition of 1.109 g (3.225 mmol) of $\text{Fe}_2\text{S}_2(\text{CO})_6$ to give a brown-gold solution. The solution was irradiated by placing the lamp 10 cm from the Pyrex Schlenk flask, the bottom half of which was immersed in the cooling bath. After irradiation for 3 h, HPLC analysis showed that $\sim 50\%$ of the C_{60} had reacted. The cloudy brown mixture was allowed to warm to room temperature and filtered. The brown filtrate was evaporated, and the residue was washed with 100 mL of hexanes to remove unreacted $\text{Fe}_2\text{S}_2(\text{CO})_6$. The residue was extracted into 15 mL of toluene and passed through a 3×45 cm column of Bio-Beads SX-3 eluting with toluene. Four bands were observed: the first was brown (higher addition products $n > 2$), the second was brown ($\text{C}_{60}[\text{S}_2\text{Fe}_2(\text{CO})_6]_2$), the third was brown ($\text{C}_{60}\text{S}_2\text{Fe}_2(\text{CO})_6$). Unreacted C_{60} (119 mg) eluted last as a purple band. The evaporated residue from the third band was recrystallized by extraction into 3 mL of CS_2 followed by the addition of 30 mL of hexanes. The brown solid was filtered off and washed with hexanes. $\text{C}_{60}[\text{S}_2\text{Fe}_2(\text{CO})_6]_2$ was worked up similarly.

$\text{C}_{60}\text{S}_2\text{Fe}_2(\text{CO})_6$: yield 132 mg (52% based on recovered C_{60}). Anal. Calcd for $\text{C}_{66}\text{Fe}_2\text{O}_6\text{S}_2$: C, 74.47; Fe, 10.49; S, 6.02. Found: C, 73.86; Fe, 10.37; H, 0.47; N, 0.0; S, 5.89. IR (CS_2): $\nu_{\text{CO}} = 2076, 2040, 2011, 2001$ cm^{-1} . UV-vis (toluene): 328 nm. FAB-MS: m/z 1065.7 ($\text{M}^+ + 1$), 1063 ($\text{M}^- - 1$). ^{13}C NMR ($\text{CS}_2/\text{benzene}-d_6$): δ 154.1, 147.5, 146.7, 146.7, 146.3, 146.0, 145.9, 145.6, 145.2, 144.6, 143.9, 143.3, 143.0, 142.4, 142.3, 140.4, 135.8. HPLC: 4.7 min.

$\text{C}_{60}[\text{S}_2\text{Fe}_2(\text{CO})_6]_2$ (at least three isomers): yield 58 mg (16% based on recovered C_{60}). Anal. Calcd for $\text{C}_{72}\text{Fe}_4\text{O}_{12}\text{S}_4$: C, 61.40; Fe, 15.86; S, 9.10. Found: C, 61.54; Fe, 14.84; H, 0.39; N, 0.07; S, 7.91. IR (CS_2): $\nu_{\text{CO}} = 2076, 2041, 2011, 2003$ cm^{-1} . UV-vis (toluene): 322 nm. FAB-MS: m/z 1408 (M^-). HPLC: 6.4, 6.9, 7.8 min.

$\text{C}_{60}[\text{S}_2\text{Fe}_2(\text{CO})_6]_3$ (at least two isomers): yield 9 mg (2% yield based on recovered C_{60}). IR (CS_2): $\nu_{\text{CO}} = 2076, 2041, 2012, 2002$ cm^{-1} . UV-vis (toluene): 318 nm. FAB-MS: m/z 1753.1 ($\text{M}^- - 1$). HPLC: 9.4, 10.3 min.

$\text{C}_{70}[\text{S}_2\text{Fe}_2(\text{CO})_6]_n$. A 250 mL Schlenk flask was charged with a 300 mg (0.357 mmol) of C_{70} and 100 mL of toluene. The clear red-violet solution was cooled to -40 °C (acetonitrile/ CO_2) followed by the addition of 534 mg (1.55 mmol) of $\text{Fe}_2\text{S}_2(\text{CO})_6$ to give a clear red-brown solution. The solution was irradiated for 2.5 h resulting in a cloudy brown mixture. This mixture was allowed to warm to room temperature and filtered, leaving a black residue. The filtrate was evaporated and the crude solid washed with 100 mL of hexanes to remove unreacted $\text{Fe}_2\text{S}_2(\text{CO})_6$. The residue was extracted into 20 mL of toluene, and this extract was passed through a 3×45 cm column of Bio-Beads SX-3 eluting with toluene. Three bands were observed:

(26) Balch, A. L.; Catalano, V. J.; Lee, J. W.; Olmstead, M. M.; Parkin, S. R. *J. Am. Chem. Soc.* **1991**, *113*, 8953.

(27) Herrmann, A.; Rüttimann, M.; Thilgen, C.; Diederich, F. *Helv. Chim. Acta* **1995**, *78*, 1673.

(28) A similar study involving nucleophilic additions to C_{70} : Karfunkel, J. H.; Hirsch, A. *Angew. Chem., Int. Ed. Engl.* **1992**, *31*, 1468; *Angew. Chem.* **1992**, *104*, 808.

(29) Lesch, D. A.; Brandt, P. F.; Stafford, P. R.; Rauchfuss, T. B. *Inorg. Synth.*, in press.

the first was brown (contained higher addition products $n \geq 3$), the second was brown ($C_{70}[S_2Fe_2(CO)_6]_2$), the third was brown ($C_{70}S_2Fe_2(CO)_6$). Unreacted C_{70} (150 mg) eluted last as red-brown band.

$C_{70}S_2Fe_2(CO)_6$: yield 136 mg (63% based on recovered C_{70}). Anal. Calcd for $C_{70}Fe_2O_6S_2$: C, 77.05; Fe, 9.43; S, 5.41. Found: C, 75.33; H, 0.10; N, <0.1. IR (CS₂): $\nu_{CO} = 2076, 2040, 2011, 2001 \text{ cm}^{-1}$. FAB-MS: m/z 1184 (M⁻). ¹³C NMR (CS₂/benzene-*d*₆): δ 160.7, 159.2, 154.0, 153.4, 151.7, 151.4, 151.1, 150.7, 150.7, 150.3 (C₇₀), 149.9, 149.6, 149.6, 149.4, 149.4, 149.2, 149.1, 149.0, 148.7, 148.3, 147.6 (C₇₀), 147.2, 147.0, 147.0 (C₇₀), 146.3, 145.7, 145.6, 145.2 (C₇₀), 143.7, 143.6, 143.4, 141.7, 140.7, 140.1, 139.7, 136.8, 133.6*, 133.4, 132.5, 132.2, 131.8, 131.6, 131.4 (C₇₀), 129.2*, 128.5*, 125.6* (* = toluene). HPLC: 7.2 min.

$C_{70}[S_2Fe_2(CO)_6]_2$ (at least four isomers): yield 110 mg (20% based on recovered C_{70}). Anal. Calcd for $C_{82}Fe_4O_{12}S_4$: C, 64.43; Fe, 14.61; S, 8.39. Found: C, 63.88; H, 0.32; N, 0.0. IR (CS₂): $\nu_{CO} = 2076, 2041, 2011, 2003 \text{ cm}^{-1}$. UV-vis (toluene): 312 nm. FAB-MS: m/z 1528 (M⁻). HPLC: 11.3, 12.2, 12.9, 14.4 min.

$C_{70}[S_2Fe_2(CO)_6]_3$ (at least three isomers): yield 65 mg (19% based on recovered C_{70}). IR (CS₂): $\nu_{CO} = 2076, 2041, 2012, 2002 \text{ cm}^{-1}$. UV-vis (toluene): 316 nm. FAB-MS: m/z 1872 (M⁻). HPLC: 17.3, 18.6, 20.3 min.

Attempted Reaction of C_{60}^- with $Fe_2S_2(CO)_6$. A 100-mL Schlenk flask was charged with 8 mg (0.04 mmol) of cobaltocene and 10 mL of toluene to give a red-orange solution. The cobaltocene-toluene solution was treated with 33 mg (0.047 mmol) of C_{60} resulting in a black precipitate and a pale yellow solution. After 2 h, 17 mg (0.049 mmol) of $Fe_2S_2(CO)_6$ was added to the clear solution. After 1 h, 12 mg (0.05 mmol) of I_2 was added to the solution. HPLC of the solution showed C_{60} and $Fe_2S_2(CO)_6$.

$Fe_2S_2(CO)_5(PPh_3)$. A 250-mL Schlenk flask was charged with 2.175 g (6.325 mmol) of $Fe_2S_2(CO)_6$ and 150 mL of THF. The clear red-orange solution was cooled to -78°C (acetone/CO₂) followed by the addition of 2.083 g (7.941 mmol) of PPh_3 and 0.578 g (5.201 mmol) of trimethylamine *N*-oxide resulting in a darkening of the solution. After 12 h, TLC showed 2 new spots with slower t_R versus the starting material. This solution was allowed to warm to room temperature and concentrated. The residue was taken up in 15 mL of 10% CH₂Cl₂/hexanes. The extract was passed through a 4 × 40 cm of silica gel column eluting with 10% CH₂Cl₂/hexanes. The red-orange band of $Fe_2S_2(CO)_6$ was followed by the red band of $Fe_2S_2(CO)_5(PPh_3)$, followed in turn by a trace amount of dark blue-red $Fe_2S_2(CO)_4(PPh_3)_2$. Yield: 3.102 g (84%). Anal. Calcd for $C_{23}Fe_2H_{15}O_5PS_2$: C, 47.78; Fe, 19.32; H, 2.61; P, 5.36; S, 11.09. Found: C, 47.94; Fe, 18.11; H, 2.86; N, 0.16; P, 5.22; S, 8.57. IR (hexanes): $\nu_{CO} = 2054, 1994, 1983 \text{ cm}^{-1}$. UV-vis (toluene): 364 nm. FD-MS: m/z 578. ¹H NMR (benzene-*d*₆): δ 7.44–7.36 (m, 6H), 7.0–6.94 (m, 9H). ¹³C NMR (benzene-*d*₆): δ 216.3–216.2 (m), 210.0 (s), 135.0 (d, $J = 41 \text{ Hz}$), 132.8 (d, $J = 11 \text{ Hz}$), 129.8 (d, $J = 2.2 \text{ Hz}$), 128.2 (d, $J = 10 \text{ Hz}$). ³¹P NMR (benzene-*d*₆): δ 60.81 (s). HPLC: 13.2 min.

(MeS)₂Fe₂(CO)₅(PPh₃). A 100-mL Schlenk flask was charged with 0.289 g (0.500 mmol) of $Fe_2S_2(CO)_5(PPh_3)$ and 40 mL of THF. The clear red-orange solution was cooled to -78°C (acetone/CO₂) followed by 1.06 mL (1.06 mmol) of 1 M LiEt₃BH. After 10 min, the resulting dark green solution was treated with 75 μL (1.20 mmol) of iodomethane. After 15 min, the dark green solution had changed to a clear red solution. After a further 1 h, the solvent was evaporated, leaving a dark red oil. This was extracted into 10% CH₂Cl₂/hexanes, and the extract was passed through a 4 × 40 cm column of silica gel eluting with the same solvent mixture to give (MeS)₂Fe₂(CO)₅(PPh₃) as a dark red band. Yield: 265 mg (87%). Anal. Calcd for $C_{25}H_{21}Fe_2O_5PS_2$: C, 49.38; H, 3.48. Found: C, 49.02; H, 3.73. IR (hexanes): $\nu_{CO} = 2038, 1971, 1921 \text{ cm}^{-1}$. UV-vis (toluene): 372 nm. FD-MS: m/z 608. ¹H NMR (benzene-*d*₆): δ 7.63 (m, 6H), 6.96 (s, 9H), 1.52 (s, *e,e* isomer), 1.45 (s, *a,e* isomer), 0.92 (s, *a,e* isomer). The *a,e:e,e* isomer ratio is 15:1. ¹³C NMR (benzene-*d*₆): δ 216.4, 210.8, 136.5 (d, $J = 38 \text{ Hz}$), 133.2 (d, $J = 11 \text{ Hz}$), 130.0 (d, $J = 1 \text{ Hz}$), 128.6 (d, $J = 9 \text{ Hz}$), 19.7, 19.0, 5.9. ³¹P NMR (benzene-*d*₆): δ 61.69 (s, *a,e* isomer), 57.07 (s, *e,e* isomer).

$C_{60}[S_2Fe_2(CO)_5(PPh_3)]_n$. A 250-mL Schlenk flask was charged with 214 mg (0.296 mmol) of C_{60} and 100 mL of toluene. The violet solution was cooled to -40°C (acetonitrile/CO₂) and treated 0.678 g (1.17 mmol) of $Fe_2S_2(CO)_5(PPh_3)$. After irradiation for 5 h, the dark

brown solution was allowed to warm to room temperature, filtered, and evaporated. The dark brown residue was washed with 100 mL of acetone to remove SPPH₃ and unreacted $Fe_2S_2(CO)_5(PPh_3)$. The residue was extracted into 15 mL of toluene and passed (in five portions) through a 3 × 45 cm column of Bio-Beads SX-3 eluting with toluene. Two bands were observed: the first was brown (containing $C_{60}[S_2Fe_2(CO)_5(PPh_3)]_2$), and the second was brown ($C_{60}S_2Fe_2(CO)_5(PPh_3)$). Unreacted C_{60} (20 mg) eluted last as a purple band.

$C_{60}S_2Fe_2(CO)_5(PPh_3)$: yield 131 mg (34%). Anal. Calcd for $C_{83}H_{15}Fe_2O_5PS_2$: C, 76.76; H, 1.16; P, 2.38; S, 4.94; Fe, 8.60. Found: C, 76.41; H, 1.45; N, 0.03; P, 2.22; S, 4.87; Fe, 8.47. IR (CS₂): $\nu_{CO} = 2045, 1995, 1980, 1943 \text{ cm}^{-1}$. UV-vis (toluene): 332 nm. FAB-MS: m/z 1298 (M⁺). ¹³C NMR (CS₂/benzene-*d*₆): δ 155.5, 155.4, 149.3, 147.5, 146.6, 146.6, 146.3, 146.2, 145.7, 145.7, 145.7, 145.6, 145.5, 145.4, 144.7, 144.4, 144.4, 143.2 (C₆₀), 143.2, 142.9, 142.9, 142.5, 142.4, 142.4, 142.4, 142.3, 140.4, 140.3, 136.3 (d, $J = 50 \text{ Hz}$), 134.4, 134.1 (d, $J = 10 \text{ Hz}$), 132.5 (d, $J = 11 \text{ Hz}$), 130.7 (d, $J = 2 \text{ Hz}$), 129.2, 128.6, 128.6, 128.5, 128.4, 128.3, 128.2, 125.6. ³¹P NMR (benzene-*d*₆): δ 66.23 (s). HPLC: 16.0 min.

$C_{60}[S_2Fe_2(CO)_5(PPh_3)]_2$: yield 181 mg (43%). Anal. Calcd for $C_{106}H_{30}Fe_4O_{10}PS_4$: C, 67.83; H, 1.61; P, 3.30; S, 6.83; Fe, 11.90. Found: C, 66.32; H, 1.86; N, 0.0; P, 3.04; S, 5.91; Fe, 11.66. IR (CS₂): $\nu_{CO} = 2044, 1985, 1970, 1942 \text{ cm}^{-1}$. UV-vis (toluene): 330 nm. FAB-MS: m/z 1876 (M⁺). ³¹P NMR (benzene-*d*₆): δ 66.58–66.21 (m). HPLC: 16.8 min.

Crystallographic Characterization of $C_{60}S_2Fe_2(CO)_6$. The gold-brown single crystals were grown by vapor diffusion of pentane into a saturated toluene/CS₂ (10:1) solution. The opaque, prismatic data crystal was mounted using Paratone oil to a thin glass fiber. The data crystal was bound by the (101), ($\bar{1}0\bar{1}$), ($1\bar{1}\bar{1}$), ($\bar{1}11$), (01 $\bar{1}$), and (0 $\bar{1}1$) faces. Distances from the crystal center to these facial boundaries were 0.11, 0.11, 0.12, 0.12, 0.13, and 0.13 mm, respectively. Data was measured at 198 K on an Enraf-Nonius CAD4 diffractometer. Crystal and refinement details are given in Table 3. Systematic conditions suggested the space group $R3m$; refinement confirmed the absence of a symmetry center. Three standard intensities monitored every 90 min showed no decay of the crystal. Step-scanned intensity data were reduced by profile analysis³⁰ and corrected for Lorentz-polarization effects and for absorption. Scattering factors and anomalous dispersion terms were taken from standard tables.³¹

The structure was solved by the direct methods;³² correct positions for Fe and S atoms were reduced from an *E* map. Subsequent cycles of isotropic least-squares refinements followed by an unweighted difference Fourier synthesis revealed positions for all the C atoms. Mirror symmetry was imposed on the Fe complex; atoms S(1), S(2), C(4), C(5), C(33), and C(34) were located on the mirror plane. 3m symmetry was imposed on the disordered toluene solvate. Two disordered pentane molecules were also present in the crystal. Successful convergence of the full-matrix least-squares refinements on F^2 was indicated by the maximum shift/error for the last cycle.³³ The highest peaks in the final difference Fourier map were observed in the vicinity of the atoms of the disordered pentane molecule; the final map had no other significant features. A final analysis of the variance between the observed and calculated structure factors showed no dependence on amplitude or resolution.

Acknowledgment. This research was supported by the National Science Foundation. We thank Scott R. Wilson for his assistance in refining the crystallographic data presented in this paper.

Supporting Information Available: Listings of atomic coordinates, thermal parameters, bond lengths, bond angles, and torsion angles (13 pages). Ordering information is given on any current masthead page.

IC960728+

(30) Coppens, P.; Blessing, R. H.; Becker, P. J. *Appl. Crystallogr.* **1972**, 7, 488.

(31) Wilson, A. J. C., Ed. *International Tables for X-ray Crystallography*; Kluwer Academic Publishers: Dordrecht, The Netherlands, 1992; Vol. C: (a) scattering factors, pp 500–502; (b) dispersion corrections, pp 219–222.

(32) Sheldrick, G. M. SHELX-86. *Acta Crystallogr.* **1990**, A46, 467. Egert, E.; Sheldrick, G. M. *Acta Crystallogr.* **1985**, A41, 262.

(33) Sheldrick, G. M. SHELX-93.